

# All-Optical Sampling Using Nonlinear Polarization Rotation in a Single Semiconductor Optical Amplifier\*

Zhang Shangjian<sup>†</sup>, Zhang Qianshu, Li Heping, Liu Yongzhi, and Liu Yong

(Key Laboratory of Broadband Optical Fiber Transmission & Communication Networks, Ministry of Education, Opto-Electronic Information School, University of Electronic Science & Technology of China, Chengdu 610054, China)

**Abstract:** We propose a novel all-optical sampling method using nonlinear polarization rotation in a semiconductor optical amplifier. A rate-equation model capable of describing the all-optical sampling mechanism is presented in this paper. Based on this model, we investigate the optimized operating parameters of the proposed system by simulating the output intensity of the probe light as functions of the input polarization angle, the phase induced by the polarization controller, and the orientation of the polarization beam splitter. The simulated results show that we can obtain a good linear slope and a large linear dynamic range, which is suitable for all-optical sampling. The operating power of the pump light can be less than 1mW. The presented all-optical sampling method can potentially operate at a sampling rate up to hundreds GS/s and needs low optical power.

**Key words:** optical signal processing; all-optical sampling; semiconductor optical amplifier; nonlinear polarization rotation

**PACC:** 4255P; 4265; 4225J

**CLC number:** TN245

**Document code:** A

**Article ID:** 0253-4177(2008)06-1031-05

## 1 Introduction

All-optical signal processing technologies are considered a possible long-term route in the evolution of telecommunication networks and high-speed signal processing systems<sup>[1]</sup>. In all-optical signal processing, all-optical analog-to-digital (A/D) conversion plays an essential role eliminating the bottleneck of electrical-to-optical and optical-to-electrical conversions. The process of all-optical A/D conversion consists of all-optical sampling, quantizing, and coding, in which the sampling rate determines the potential for A/D conversion<sup>[2-8]</sup>. Many techniques, such as self-and cross-phase modulation (SPM, XPM)<sup>[2,7]</sup>, four wave mixing (FWM)<sup>[9]</sup>, and the Raman soliton self-frequency shifting in fibers, have been employed to realized all-optical sampling functions<sup>[3,5]</sup>. However, these examples are based on the nonlinear effects in fiber or other materials. They also require tens of kilometers of high nonlinearity fiber and high power optical pulses to induce enough nonlinear effects, which is not suitable for integrated signal process devices. Moreover, it is difficult to control the relationships between the sampling optical pulses and the analog

optical signals accurately in practice, and, therefore, only 3 bit resolution for these A/D converters has been reported<sup>[5,6]</sup>.

Recently, considerable attention has been paid to optical signal processing based on nonlinear polarization rotation (NPR) in semiconductor optical amplifiers (SOAs). The use of polarization switches based on NPR in SOAs in optical signal processing applications is receiving considerable interest by many research groups<sup>[10-15]</sup>. Applications of polarization switches based on NPR in SOAs to wavelength conversion, all-optical flip-flop memories, and optical time domain demultiplexing are presented in Refs. [11,12,15].

In this paper, we investigate NPR in an SOA in the context of all-optical sampling. We show that the polarization-dependent gain saturation model presented in Ref. [12] can be applied to describe optical sampling in an SOA. In the case of optical sampling, the role of the saturating control beam is taken over by the analog signal optical light, and the probe light is replaced by the high-speed optical clock pulses train. The feasibility of the scheme is numerically demonstrated. We also investigate the optimized operating parameters of the proposed system by simulating

\* Project supported by the National Natural Science Foundation of China (No. 60736038), the National High Technology Research and Development Program of China (No. 2007AA01Z269), the National Defense Pre-Research Foundation of China (No. 51302060101), and the Program for New Century Excellent Talents in University (No. NCET-06-0805)

<sup>†</sup> Corresponding author. Email: sjzhang@uestc.edu.cn

Received 29 December 2007

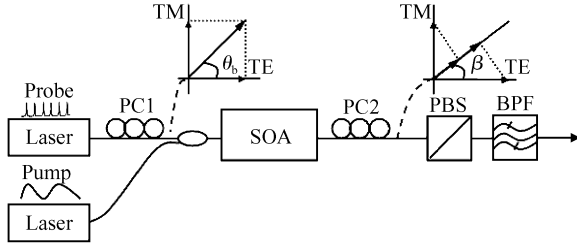


Fig.1 Scheme of the all-optical sampling based on nonlinear polarization rotation

the output intensity of the probe light as functions of the input polarization angle, the phase induced by the polarization controller, and the orientation of the polarization beam splitter. The simulated results show that we can obtain a good linear slope and a large linear dynamic range, which is suitable for all-optical sampling. The operating power of the pump light can be less than 1mW. The presented all-optical sampling method can potentially operate at a sampling rate up to hundreds of GS/s and needs low optical power. The proposed sampling scheme is compatible with the optical networks and allows photonic integration.

## 2 Operating principle

The underlying concept of NPR driven by polarization-dependent gain saturation in an SOA was presented in Refs. [11~13]. In brief, the polarization rotation operates in a similar fashion to the Mach-Zehnder interference, but the role of the different arms is taken over by the transverse electric (TE) and transverse magnetic (TM) modes of the incoming coherence light. The modes propagate independently through the SOA, but they have indirect interaction via the carriers. The TE and TM modes couple to two different reservoirs of holes. Thus, if the SOA is saturated by an optical control signal, the gain saturation of the TE mode differs from that of the TM mode. Hence, the refractive index change of the TE mode also differs from that of the TM mode. If a small probe light with well-defined polarization is simultaneously injected into the SOA with a saturating pump light, a phase difference between the two modes builds up as the probe light propagates through the SOA. When the two modes recombine at the polarization beam splitter (PBS), the phase difference determines to which of the output ports of the PBS the signal is switched.

The principle of polarization-dependent SOA gain was applied to a nonlinear polarization switch<sup>[12]</sup>. In this work, we will use it to realize an all-optical sampling function. The general scheme of the

all-optical sampling is depicted in Fig. 1. The sampler is made from an SOA, two polarization controllers (PCs), an optical band pass filter (BPF), and a polarization beam splitter (PBS). The continuous-wave (CW) optical signal at wavelength  $\lambda_p$  that needs to be sampled is injected into the SOA as the pump light, and, in the meantime, optical clock pulses train at wavelength  $\lambda_b$  are injected into the SOA as the probe light. This configuration is different from that in PSW. The output of the SOA is fed into a PBS and the probe light ( $\lambda_b$ ) is filtered through the BPF. The system contains two polarization controllers. The first polarization controller (PC1) adjusts the polarization of the probe light to an appropriate angle to the orientation of the SOA layers, while the second polarization controller (PC2) adjusts the polarization of the amplified probe light to the orientation of the PBS. When the SOA gain is saturated by the injected high-intensity pump light, the polarization state of the probe light will be rotated due to the birefringence of the SOA, and the polarization rotating angle of probe light can be controlled by the intensity of the pump light. If the intensity of the pump light carries signals, then the signals are passed onto the pulsed probe light through the controlled polarization rotating. Thus, all-optical sampling is obtained.

We decompose the incoming arbitrarily polarized electric field in a component parallel to the layers in the waveguide (TE mode) and a perpendicular component (TM mode). These two polarization directions are along the principal axes that diagonalize the wave propagation in the SOA. In the case of all-optical sampling, it is not necessary to account for the ultrafast (subpicosecond timescale) intraband relaxation dynamics. The propagation equation for the TE- and TM-polarized electric field component is<sup>[12,13]</sup>

$$\left(\frac{\partial}{\partial t} + v_g^i \frac{\partial}{\partial z}\right) A^i(z, t) = \frac{1}{2} \Gamma^i (1 + j\alpha^i) g^i A^i(z, t) - \frac{1}{2} \alpha_{\text{int}}^i A^i(z, t), \quad i = \text{TE or TM} \quad (1)$$

where the superscript  $i = \text{TE and TM}$  correspond to TE mode and TM mode, respectively.  $A(z, t)$  is the weakly time and space-dependent complex envelope of the optical field,  $v_g$  is the corresponding group velocity taken at the central frequency of the wave,  $\Gamma$  is the confinement factor,  $g$  is the gain and assumed to be constant along the light propagation in the SOA,  $\alpha$  is the phase-modulation parameter, and  $\alpha_{\text{int}}$  is the modal loss. The envelopes for each polarization can be expressed as

$$A^i(z, t) = \sqrt{S^i(z, t)} e^{j\varphi^i(z, t)}, \quad i = \text{TE or TM} \quad (2)$$

Here,  $S(z, t)$  and  $\varphi(z, t)$  represent the photon numbers and phases, respectively. From Eq. (1), the net

amplifications and the difference in phase between TE and TM components when light goes through the SOA can be written as

$$G^i = \exp\left[(\Gamma^i g^i - \alpha_{\text{int}}^i) \frac{L}{v_g}\right], \quad i = \text{TE or TM} \quad (3)$$

$$\Delta\varphi = \varphi^{\text{TE}} - \varphi^{\text{TM}} = \frac{1}{2} \left( \frac{\alpha^{\text{TE}} \Gamma^{\text{TE}} g^{\text{TE}}}{v_g^{\text{TE}}} - \frac{\alpha^{\text{TM}} \Gamma^{\text{TM}} g^{\text{TM}}}{v_g^{\text{TM}}} \right) \quad (4)$$

The two optical modes have indirect interaction via the carriers. It is assumed that the TE and TM polarizations couple the electrons in the conduction band with two distinct reservoirs of holes<sup>[12]</sup>. If the number of electrons in the conduction band is denoted by  $n_c(z, t)$ , and the number of holes involved in the  $x$  and  $y$  transitions is denoted by  $n_x(z, t)$  and  $n_y(z, t)$ , we have

$$n_c(z, t) = n_x(z, t) + n_y(z, t) \quad (5)$$

Since we do not consider applications that involve ultrafast dynamics here, the two populations  $n_x$  and  $n_y$  will be clamped tightly together, i. e.,

$$n_x(z, t) = f n_y(z, t) \quad (6)$$

where  $f$  is the hole population imbalance factor representing the anisotropy magnitude of the SOA. In the case of unstrained bulk material, the gain will be isotropic and  $f = 1$ . In the case of tensile strain, TE gain will be larger than TM, i. e.,  $f < 1$ . The (linearized) gain  $g^{\text{TE/TM}}$  can be written as

$$g^{\text{TE}} = \xi^{\text{TE}} (n_c + n_x - n_0) V_a \quad (7a)$$

$$g^{\text{TM}} = \xi^{\text{TM}} (n_c + n_y - n_0) / V_a \quad (7b)$$

where  $\xi^{\text{TE}}$  and  $\xi^{\text{TM}}$  are the gain coefficients for the TE and TM modes, respectively,  $n_0$  is the total number of electronic states involved in the optical transition, and  $V_a$  is the active region volume of SOA.

When the pump and probe lights inject in the SOA, the rate equation is given below, assuming that the effects of spontaneous emission and residual facet reflectivities are negligible.

$$\frac{dn_x}{dt} = \frac{f}{1+f} \times \frac{I}{q} - \frac{n_x}{\tau_c} - \Gamma^{\text{TE}} g^{\text{TE}} \frac{G^{\text{TE}} - 1}{\Gamma^{\text{TE}} g^{\text{TE}} - \alpha_{\text{int}}^{\text{TE}}} \times \left( \frac{P_b}{h\nu_b} \cos^2 \theta_b + \frac{P_p}{h\nu_p} \cos^2 \theta_p \right) \quad (8a)$$

$$\frac{dn_y}{dt} = \frac{f}{1+f} \times \frac{I}{q} - \frac{n_y}{\tau_c} - \Gamma^{\text{TM}} g^{\text{TM}} \frac{G^{\text{TM}} - 1}{\Gamma^{\text{TM}} g^{\text{TM}} - \alpha_{\text{int}}^{\text{TM}}} \times \left( \frac{P_b}{h\nu_b} \sin^2 \theta_b + \frac{P_p}{h\nu_p} \sin^2 \theta_p \right) \quad (8b)$$

where  $I$  is the pump electric current injected in SOA,  $q$  is the electric unit charge,  $\tau_c$  is the electron-hole recombination time,  $h$  is the Planck's constant,  $\nu_b$  and  $\nu_p$  are the frequencies of the probe light and pump light, respectively, and  $\theta_b$  and  $\theta_p$  are the input polarized angles of probe light and pump light related to the orientation of the SOA layers, respectively.

As is shown in Fig. 1, the two modes' components of probe light that are parallel to the PBS orien-

Table 1 Definition of SOA parameters

Definition	Parameter	Value	Unit
Active region length	$L$	800	$\mu\text{m}$
Active region area	$A$	0.2	$\mu\text{m}^2$
Active region volume	$V_a$	160	$\mu\text{m}^3$
Confinement factor	$\Gamma^{\text{TE}}, \Gamma^{\text{TM}}$	0.2, 0.14	
Phase modulation coefficients	$\alpha^{\text{TE}}, \alpha^{\text{TM}}$	5, 5	
Modal loss	$\alpha_{\text{int}}^{\text{TE}}, \alpha_{\text{int}}^{\text{TM}}$	$2.7 \times 10^3$	$\text{m}^{-1}$
Gain coefficients	$\xi^{\text{TE}}, \xi^{\text{TM}}$	$2.5 \times 10^{-20}$	$\text{m}^2$
Hole population imbalance factor	$f$	0.5	
Electron-hole recombination time	$\tau_c$	500	ps
Optical transition state number	$N_0$	$2 \times 10^8$	
Group velocity	$v_g$	80	$\mu\text{m}/\text{ps}$
Electrical current	$I$	160	mA

tation combine. Since these components are coherent, they will interfere with each other. Therefore, the optical intensity of probe light that passes through the PBS is given by

$$S_{\text{bout}} = S_{\text{bout}}^{\text{TE}} + S_{\text{bout}}^{\text{TM}} + 2\sqrt{S_{\text{bout}}^{\text{TE}} S_{\text{bout}}^{\text{TM}}} \cos(\Delta\varphi + \phi_{\text{pc}}) \quad (9a)$$

$$S_{\text{bout}}^{\text{TE}} = \frac{P_b}{h\nu_b} \times \frac{L}{v_g^{\text{TE}}} \cos^2 \theta_b \cos^2 \beta G^{\text{TE}} \quad (9b)$$

$$S_{\text{bout}}^{\text{TM}} = \frac{P_b}{h\nu_b} \times \frac{L}{v_g^{\text{TM}}} \sin^2 \theta_b \sin^2 \beta G^{\text{TM}} \quad (9c)$$

In Eq. (9),  $\phi_{\text{pc}}$  is a phase induced by the PC2 and  $\beta$  is the angle between the orientation of the PBS and the SOA layers.

In our optical sampling model, the pump light carrying signals creates a modulated phase difference ( $\Delta\varphi$ ) between the TE and TM mode of probe light. Equation (9) shows that the change of pump light power alters the  $\Delta\varphi$ , thus altering the output intensity of the probe light. When the probe light is the train of optical clock pulses, its envelope will vary with the input power of the pump light. In this way, signals carried by the pump light are delivered to the optical clock pulses, and thus all-optical sampling operation can be achieved.

### 3 Simulated results

Several important characteristics of our proposed sampler can be investigated by solving Eqs. (3)~(9). In order to sample signals accurately, it is necessary to obtain the non-invert transfer curve (output probe light power versus input pump light power) and determine the static operating point. All the parameters of the SOA are listed in Table 1. In the simulation, the wavelength of the probe light is  $1.55 \mu\text{m}$ , the light power is invariable at  $0.126 \text{mW}$  ( $-9 \text{dBm}$ ), and the wavelength of the pump light is  $1.59 \mu\text{m}$ . The rotated polarization angle induced by NPR versus the input polarized angle of the probe light is obtained and shown in Fig. 2. This figure shows that the maximum birefringent effect can be obtained when the input

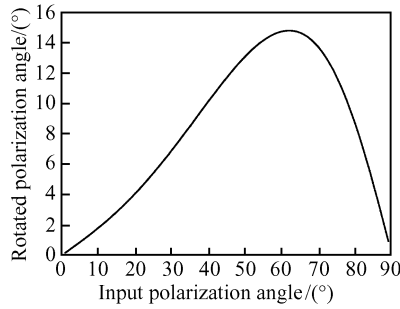


Fig. 2 Computed rotated polarization angle as a function of the input polarization angle of a probe light SOA was pumped with 160mA.

polarized angle of probe light is approximately  $62^\circ$ , which indicates the optimum orientation of PC1.

Next, the PC2 are set in such a way that the probe can not pass through the PBS if only the probe light is present. If a saturating pump beam is coupled into the SOA, the additional birefringence in the SOA leads to a phase difference between TE and TM modes of the probe light, causing the polarization of the probe light to be rotated. As a consequence, some probe light can pass through the PBS. Hence, an increase in the intensity of the pump light leads to an increase in the intensity of the probe light that outputs through the PBS. Thus, the optical sampling is obtained. As shown in Fig. 3, when  $\phi_{pc} = 21^\circ$  and  $\beta =$

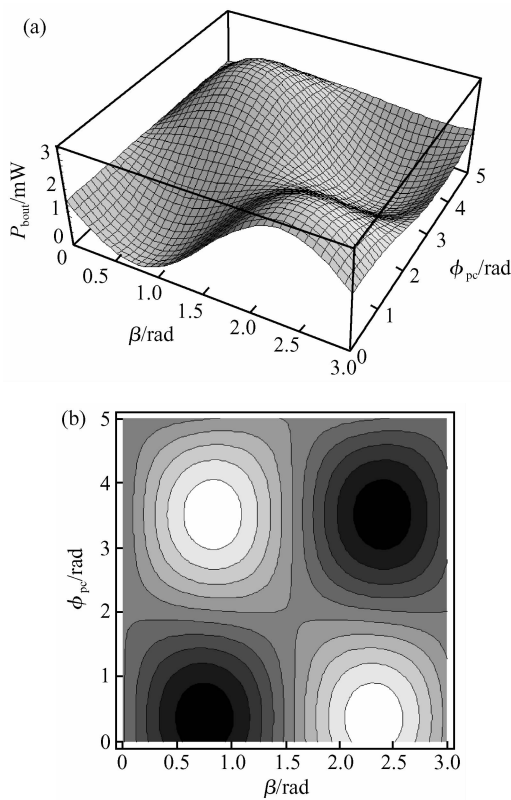


Fig. 3 (a) Intensity of probe light that outputs through the PBS as functions of the phase induced by the PC2 and the orientation of the PBS; (b) Contour of (a)

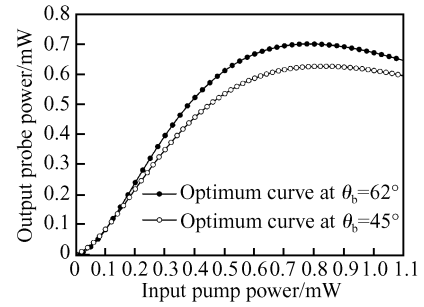


Fig. 4 Non-invert transfer curves of SOA at different input probe lights

$43^\circ$ , the intensity of the probe light that outputs through the PBS reaches its minimum.

The optimum transfer curve can be achieved at the condition of  $I = 160\text{mA}$ ,  $\theta_b = 62^\circ$ ,  $\phi_{pc} = 21^\circ$ , and  $\beta = 43^\circ$ , which is shown in Fig. 4. The transfer curve at the input polarization angle  $45^\circ$  is also given in the figure for comparison. From Fig. 5, we can see that the slope and linear range of the transfer curve at  $\theta_b = 62^\circ$  is superior to that at  $\theta_b = 45^\circ$ , which differs from the denotation by many that the maximum birefringent effect is achieved at the input angle of approximately  $45^\circ$ , and finds the optimized input angle is necessary to improve the sampling accuracy.

When the intensity of the time-varying pump light ranges from 0.1mW to 0.6mW, the linearity of the transfer curve is better and the sampling result will be more accurate. The sampling results of our all-optical sampling model are shown in Fig. 5. When the time-varying optical signal and timing optical clock pulses are injected into the SOA, representing pump light and probe light, respectively, the power of the pump light controls the intensity of the output optical pulse by controlling the rotated angle of the NPR of the optical pulse. As the clock optical probe light pulses pass through the SOA, the sampling signals are delivered from the pump light to the optical clock pulses. As is shown in Fig. 5, the maximum power needed in the sampling process is 0.5mW, which is much lower than other sampling methods mentioned in Refs. [2~8].

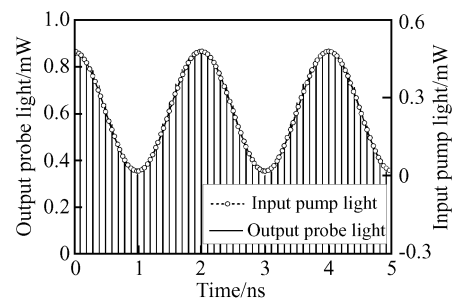


Fig. 5 Sampling result with all-optical sampling model

The sampling process of our scheme is switching signals from pump light at wavelength  $\lambda_p$  to the optical clock pulses at wavelength  $\lambda_b$  through the NPR of SOA, which is similar to the processing of wavelength conversion. Since it has been demonstrated experimentally that the SOA-based wavelength conversion can reach the operating speed of 320 Gbit/s<sup>[15]</sup>, it can be predicted that the sampling rate of our method could also operate at a similar speed.

## 4 Conclusion

We have presented a simple rate-equation model that is capable of describing the all-optical sampling scheme using nonlinear polarization rotation in an SOA. The feasibility of the proposed scheme has been proved by the numerical investigation. The simulation results also show that the maximum optical operating power required in our scheme is less than 1mW. The sampling rate promises to reach several hundred GS/s. Furthermore, the sampling devices are compatible with optical networks and suitable for integration.

## References

- [1] Calabretta N, Liu Y, Huijskens F M, et al. Optical signal processing based on self-induced polarization rotation in a semiconductor optical amplifier. *J Lightwave Technol*, 2004, 22(2):372
- [2] Ho P P, Wang Q Z, Chen J, et al. Ultrafast optical pulse digitization with unary spectrally encoded cross-phase modulation. *Appl Opt*, 1997(36):3425
- [3] Konishi T, Tanimura K, Asano K. All-optical analog-to digital converter by use of self-frequency shifting in fiber and a pulse-shaping technique. *J Opt Soc Am B*, 2002, 19:2817
- [4] Xu C, Liu X. Photonic analog-to-digital converter using soliton self-frequency shift and interleaving spectral filters. *Opt Lett*, 2003, 28:986
- [5] Oda S, Maruta A. 2-bit all-optical analog-to-digital conversion by slicing supercontinuum spectrum and switching with nonlinear optical loop mirror and its application to quaternary ASK-to-OOK modulation format converter. *IEICE Trans Commun*, 2005, E88-B(5):1963
- [6] Ikeda K, Abdul J M, Tobioka H, et al. Design considerations of all-optical A/D conversion; nonlinear fiber-optic Sagnac-loop interferometer-based optical quantizing and coding. *J Lightwave Technol*, 2006, 24(7):2618
- [7] Oda S, Maruta A. Two-bit all-optical analog-to-digital conversion by filtering broadened and split spectrum induced by soliton effect or self-phase modulation in fiber. *IEEE J Sel Topics Quantum Electron*, 2006, 12(2):307
- [8] Nishitani T, Konishi T, Itoh K. All-optical analog-to-digital conversion using optical delay line. *IEICE Trans Electron*, 2007, E-90-C:479
- [9] Oda S, Mao X L, Maruta A, et al. All-optical analog-to-digital conversion based on fiber nonlinearity. *Electron Commun in Japan*, 2005, 88:116
- [10] Nishitani T, Konishi T, Itoh K. Integration of a proposed all-optical analog-to-digital converter using self-frequency shifting in fiber and a pulse-shaping technique. *Opt Rev*, 2005, 12:237
- [11] Liu Y, Hill M T, Tangdiongga E, et al. Wavelength conversion using nonlinear polarization rotation in a single semiconductor optical amplifier. *IEEE Photonics Technol Lett*, 2003, 15(1):90
- [12] Dorren H J S, Lenstra D, Liu Y, et al. Nonlinear polarization rotation in semiconductor optical amplifiers: theory and application to all-optical flip-flop memory. *IEEE J Quantum Electron*, 2003, 39(1):141
- [13] Yang X, Lenstra D, Khoea G D, et al. Nonlinear polarization rotation induced by ultrashort optical pulses in a semiconductor optical amplifier. *Opt Commun*, 2003, 223:169
- [14] Hill M T, Tangdiongga E, de Waardt H, et al. Carrier recovery time in semiconductor optical amplifiers that employ holding beams. *Opt Lett*, 2002, 27(18):1625
- [15] Liu Y, Tangdiongga E, Li Z, et al. Error-free 320Gb/s all-optical wavelength conversion using a single semiconductor optical amplifier. *J Lightwave Technol*, 2007, 25(1):103

## 基于半导体光放大器非线性偏振旋转效应的全光采样\*

张尚剑<sup>†</sup> 张谦述 李和平 刘永智 刘永

(宽带光纤传输与通信教育部重点实验室, 电子科技大学光电信息学院, 成都 610054)

**摘要:** 提出了一种新的基于半导体光放大器非线性偏振旋转效应的全光采样方法, 利用速率方程对全光采样的理论机理进行了阐述. 借助该速率方程模型对采样器的输入偏振角、偏振控制器的附加相移和偏振合束器的偏振方向等参数进行了优化设计. 计算结果表明, 采样器传输曲线具有较好的线性工作范围, 能够实现模拟光信号的高速全光采样, 且其输入泵浦光功率小于 1mW. 由于该全光采样的工作原理与全光波长转换类似, 而目前的全光波长转换工作速率可达 320Gbps, 因此该全光采样的采样速率可望达到上百 GS/s.

**关键词:** 光信号处理; 全光采样; 半导体光放大器; 非线性偏振旋转

**PACC:** 4255P; 4265; 4225J

**中图分类号:** TN245

**文献标识码:** A

**文章编号:** 0253-4177(2008)06-1031-05

\* 国家自然科学基金(批准号:60736038), 国家高技术研究发展计划(批准号:2007AA01Z269), 国防预研基金(批准号:51302060101)和新世纪优秀人才计划(批准号:NCET-06-0805)资助项目

<sup>†</sup> 通信作者. Email: sjzhang@uestc.edu.cn

2007-12-29 收到